Journal of Superconductivity: Incorporating Novel Magnetism, Vol. 16, No. 5, October 2003 (© 2003)

Linear-Defect-Induced Thermal Instability in YBCO Thin Films in Microwave Fields

V. M. Pan,[1] C. G. Tretiatchenko,[1] V. S. Flis,[1] V. A. Komashko,[1] O. A. Kalenyuk,[1] E. A. Pashitskii,[2] A. N. Ivanyuta,[3] G. A. Melkov,[3] H. W. Zandbergen,[4] and V. L. Svetchnikov,[4]

Received September 30, 2002

An induced heat instability proposed to explain the difference between microwave properties of YBCO single crystals and thin films at temperatures just below T_c. Extended strain fields near out-of-plane edge dislocations are initial discontinuities for the instability development. We have shown theoretically and have confirmed experimentally that a single dislocation can not have a strong effect on the microwave surface resistance R_s. Dislocation arrays, which were observed experimentally, can induce the thermal instability if edge dislocations in the arrays are spaced closer than the heat relaxation length. Ordered dislocation structures provide much higher local temperature perturbation than randomly distributed dislocations.

KEY WORDS: edge dislocations; heat instability; high-temperature superconducting epitaxial thin films; microwave surface resistance.

1. INTRODUCTION

Microwave properties of high-temperature superconductors (HTS) cause a great interest because of their significance for multiple applications, especially in wireless communication technologies, as well as of the physics involved.

The anomalous microwave behavior of HTS includes their strong nonlinearity at rather low microwave power [1], which is a severe obstacle for HTS application, and the anomalous temperature dependence of surface resistance R_s with a wide peak near about 40 K [2]. Moreover, this peak is not fully reproducible for different kinds of samples (films and single crystals) and procedures of their preparation. Several approaches are usually used to explain anomalous behavior of the surface impedance of YBCO films: the $d_{x^2-y^2}$ symmetry of superconducting order parameter [3,4], weak links between crystallites [5], and influence of oxygen stoichiometry and point defects [6].

Peculiarities of microwave behavior at temperatures near the temperature of superconducting transition, T_c, may have even more significance as practical applications. HTS devices and components work usually at the temperature of liquid nitrogen of 77 K, rather close to T_c. In this temperature range, thermal effects can have a great influence on microwave properties.

We suggest that a thermal instability, which may develop in the films not far below T_c at high microwave power, can be the reason of anomalous temperature behavior of the microwave surface resistance and nonlinear effects. The main objective of the present work is to analyze linear defects as a possible intrinsic source of the instability.

2. SAMPLES AND STRUCTURE

A set of samples (more than 10) has been prepared to check the influence of linear defects on microwave properties of HTS films. $YBa_2Cu_3O_{7-\delta}$ (YBCO) films were deposited over a CeO_2 buffer

[1]Department of Superconductivity, Institute for Metal Physics, Kyiv 03142, Ukraine.
[2]Institute of Physics, Kyiv 03022, Ukraine.
[3]Department of Cryo- and Microelectronics, T. Shevchenko National University, Kyiv 03127, Ukraine.
[4]National Centre for HREM, TU Delft, 2628 AL Delft, The Netherlands.

0896-1107/03/1000-0889/0 © 2003 Plenum Publishing Corporation

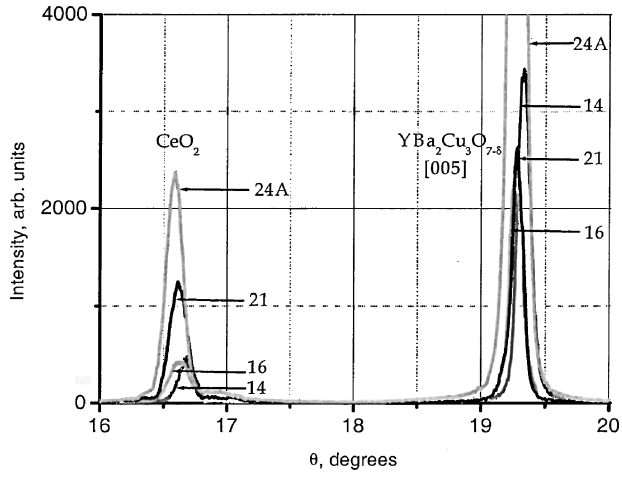

Fig. 1. Fragment of θ–2θ scan for $YBa_2Cu_3O_{7-x}$ films on sapphire substrates with CeO_2 barrier layers. The temperatures of CeO_2 deposition: 14 – 960°C; 16 – 865°C; 21 – 780°C; 24A – 915°C.

layer onto sapphire substrates by off-axis RF magnetron sputtering [7]. All the films were *c*-oriented and about 300 nm thick.

To achieve just very small difference between the samples, only in their dislocation structure, all parameters of YBCO deposition (substrate temperature of about 740°C, magnetron power, oxygen pressure, time of deposition) were absolutely the same for the majority of samples. The only variation in sample preparation procedure was the substrate temperature during preparation of the CeO_2 sublayer, which was ranged from 780 to 960°C. The structure of samples was examined by X-ray diffraction ((00*l*)-peaks were checked). Uncontrollable variations of deposition regime were not completely eliminated. So, preliminary X-ray characterization was found to be extremely important. We eliminated from the sample set all samples containing any *a*-oriented phase. A lower quality of the buffer layer (produced at lower temperature) resulted usually in slightly wider X-ray peaks both for CeO_2 and for YBCO. A larger number of substrate-induced dislocations as well as smaller domain size in the YBCO could be expected for the samples produced with lower buffer layer deposition temperatures.

A fragment of θ–2θ scan for four typical $YBa_2Cu_3O_{7-x}$ films is shown in Fig. 1. The reflection angles and widths of CeO_2 and YBCO (005) peaks for these samples are given in Table I. Peaks were Gaussian fitted and the parameters were extracted by Levenberg–Marquardt iteration procedure. Note that the sample N16 has essentially wider CeO_2 peak and slightly wider and distorted YBCO (005) peak compared to other ones.

More detailed X-ray studies of YBCO films were carried out with a four-circle diffractometer [8]. The samples were rotated step-by-step or continuously around three orthogonal axes α, β, θ, Depending on the certain task the step of movement was changed from 3′ up to 2°. Scanning over an area 0.25–40 mm^2 was made with fixed recording geometry. $Cu_{K\alpha}$ radiation was used with a LiF monochromator. The system of slits for incident and reflected beams created a divergence lower than 0.04–0.06°. The size of simultaneously irradiated area was varied from 0.25×0.25 to 0.25×8.0 mm^2. The reflection intensity $I(q)$ (q is a vector in reciprocal space) was recorded in each point of the area with increased intensity $I(q)$ near a reciprocal lattice point. So, the full $I(q)$ distribution was obtained. The distributions in both planes parallel and perpendicular to the diffraction vector, $I(q\|)$ and $I(q\perp)$, could be plotted.

X-ray analysis of the intensity distribution around reflection (005) was performed for the YBCO films deposited at different temperatures (780 and 740°C). The contour plots of $I(q_\perp)$ are shown in Fig. 2. Different film deposition regimes resulted in significantly changed shape of the isointensity lines $I(q_\perp)$. The broadening of the reflection shown in Fig. 2a has a circular symmetry, while the shape of isointensity lines in Fig. 2b is essentially elongated in ⟨100⟩ direction. We have shown earlier [9] that this could be attributed to different numbers of edge dislocations in the films.

Table I. The Reflection Angle and Width of CeO_2 and YBCO (005) Peak for the Samples Prepared at Different Substrate Temperatures T_s During Deposition of CeO_2 Buffer Layer

		CeO_2 peak		YBCO (005) peak	
Sample number	T_s (°C)	$\theta°$	$\Delta\theta°$	$\theta°$	$\Delta\theta°$
14	960	16.6844 ± 0.0006	0.127 ± 0.001	19.3317 ± 0.0003	0.1026 ± 0.0006
16	865	16.6241 ± 0.0007	0.156 ± 0.001	19.2692 ± 0.0005	0.1034 ± 0.0011
21	780	16.6169 ± 0.0005	0.137 ± 0.001	19.2812 ± 0.0006	0.0947 ± 0.0012
24A	915	16.5851 ± 0.0004	0.131 ± 0.001	19.2714 ± 0.0003	0.1063 ± 0.0005

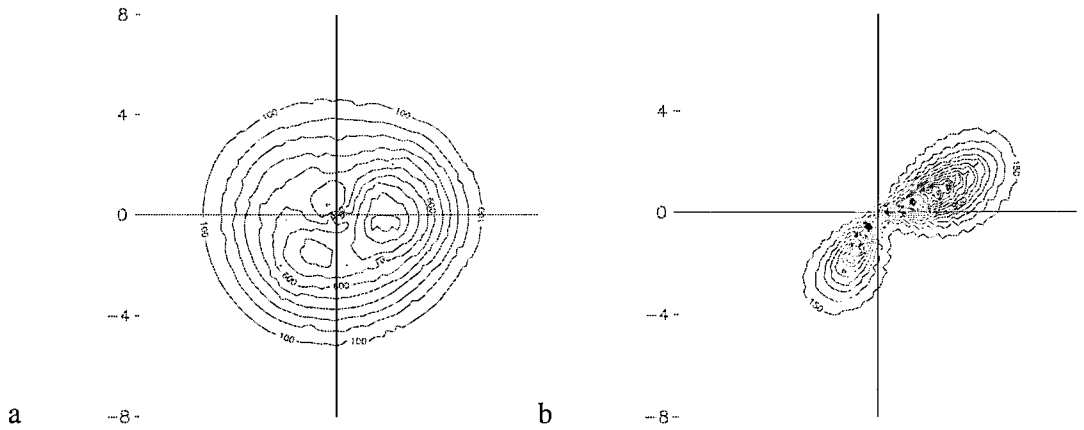

Fig. 2. Isointensity lines of $I(q_\perp)$ for $YBa_2Cu_3O_{7-\delta}$ film deposited at 780°C (a) and 740°C (b) (reflection (005)).

High-resolution electron microscopy (HREM) visualizing the locations of individual atoms, enables dislocations to be directly counted. The correlation between film growth conditions, X-ray data and the number of dislocation was qualitatively confirmed. The details of HREM studies are published elsewhere [10].

The epitaxial YBCO film growth is accompanied by arising stress–strain fields, partially relaxed by formation of dislocation arrays. There are two main types of edge dislocations arrays in YBCO films: (a) out-of-plane, associated with mosaic domains separated by low-angle tilt dislocation boundaries (typical misorientation angle is about 1–2°, typical domain size is 20–50 nm, mean dislocation spacing within a boundary is 10–20 nm, and average density of dislocations is about 10^{11} lines/cm^2); (b) in-plane, associated with misfit dislocations and dislocation loops connected with stacking faults, i.e., with segments of extra copper–oxygen layers CuO_2 or their local absence. In quality YBCO films such a very dense dislocation structure coexists with a perfect crystallinity defined by TEM/HREM and X-ray diffractometry. Screw dislocations were shown to be unable to influence microwave properties, because of much lower density and weak elastic strains [9].

The extended areas around the out-of-plane edge dislocations with completely or partially suppressed superconducting order parameter, increasing the effective density of normal carriers, are supposed to be a source of additional microwave losses. YBCO crystals have the anomalous strong T_c-dependence on the uniaxial compression stress P_i. For the optimally doped $YBa_2Cu_3O_{7-\delta}$ single crystal the derivatives $C_i = \partial T_c/\partial P_i$ were measured to be $\partial T_c/\partial P_a \approx -(1.9 \div 2)$ K/GPA, $\partial T_c/\partial P_b \approx (1.9 \div 2.2)$ K/GPa, $\partial T_c/\partial P_c \approx -(0 \div 0.3)$ K/GPa. This means that $T_c(P)$ dependence for hydrostatic compression crystal is very weak. However, the local T_c variations can be very substantial in anisotropically strained regions.

Calculations [9] have shown that elastic deformation of YBCO crystal, induced by a single out-of-plane edge dislocation or by an out-of-plane dislocation wall, results in a local reduction of T_c and complete suppression of superconducting state in some region. A normal phase area should exist around the dislocation core, which is the cylindrical channel of a plastically deformed medium with diameter of about 2 nm.

The details of calculation of T_c variation were reported earlier [9]. The equation, which determines the shape of normal phase area near the edge dislocation core:

$$r_N(\varphi, T) = R_0(T) \sin\varphi[1 + \beta_0 \cos^2\varphi] \le 0, \qquad (1)$$

where $R_0(T)$ is a characteristic size determined by the dislocation Burgers vector, $\partial T_c/\partial P_i$ derivatives, and the Poisson's coefficient. $\beta_0 = (C_a - C_b)/C_a + C_b)$ is a coefficient describing the anisotropy of T_c-dependence on stress in *ab* plane, φ is the azimuth angle in this plane.

It should be noted that the shape is very similar to the shape of isointensity lines in Fig. 2b. This is the argument that the peak broadening is directly connected with predominant edge dislocations in the film.

For a critical temperature of a nondeformed crystal $T_{c0} = 90$ K, the estimated parameters are $R_0(T) \approx 0.042/\tau$ nm ($\tau = 1 - T/T_{c0}$) and $\beta_0 \approx -24$. At $T = 77$ K this results in $R_0 \approx 0.3$ nm and the maximum r_N value

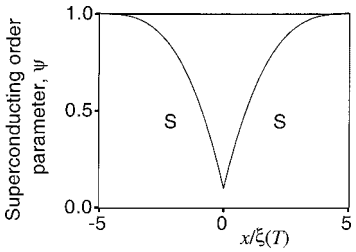

Fig. 3. The spatial distribution of superconducting order parameter in direction $\varphi = \pi/4$ calculated in [11].

is $r_{\mathrm{Nmax}} \approx 2.5$ nm. Taking into account a proximity effect, the area with suppressed T_c expands in all directions by about the coherence length $\xi(T) = \xi_0/\tau^{1/2}$ (where $\xi_0 \approx 1.3$ nm is the coherence length at $T = 0$).

The model of the spatial distribution of the superconducting order parameter, calculated in [11] and shown in Fig. 3 for direction $\varphi = \pi/4$, is invariant in $x/\xi(T)$ coordinates. Therefore, the volume fraction with suppressed order parameter is visually equivalent to the length of horizontal section in the shaded area, the section raising with the temperature.

At 77 K $\xi(T) \approx 3.5$ nm and the maximum width of the normal region is $L(T) = 2[r_{\mathrm{Nmax}} + \xi(T)] \geq 12$ nm. The area of suppressed order parameter for a single dislocation can be estimated as $S_{\mathrm{N}}(T) \approx 2\xi(T)L(T)$, that is about 8×10^{-13} cm^2 at 77 K. For the out-of-plane edge dislocation density of 10^{11} lines/cm^2 the fraction of normal phase is about 10%. This is a quite sufficient value to affect microwave losses. The $L(T)$ function components demonstrate different behavior at $T \to T_{c0}$. $r_{\mathrm{N}}(T)$ is proportional to τ^{-1} and $\xi(T)$ to $\tau^{-1/2}$. Hence, the normal phase fraction and high frequency losses increase with temperature faster than τ^{-1} and approach to $\tau^{-3/2}$ at T_{c0}. The parameter of anisotropy β_0 in Eq. (1) for the in-plane edge dislocation is several times less than that for out-of-plane edge dislocation, because of the low $\partial T_c/\partial P_c$ value, $\beta_{ac,bc} \approx 4.5$. Thus, in-plane dislocation lines and loops are unlikely to contribute noticeably to the microwave losses in contrast to the out-of-plane dislocations.

3. MICROWAVE PROPERTIES

The microwave surface resistance, $R_s(T)$, was measured in the temperature range 20–100 K with the end-plate cavity technique. The measurements were performed at fixed frequency, f, of 135 GHz. The law $R_s \propto f^2$ is no longer valid in this frequency range and

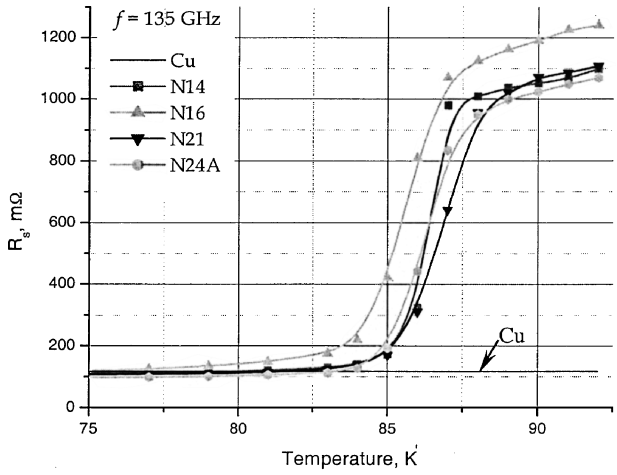

Fig. 4. Surface resistance of YBCO films in the high temperature range. The surface resistance of pure copper at the same frequency is shown for comparison.

R_s of Cu is just slightly higher than R_s of YBCO in superconducting state. The experimental temperature dependencies $R_s(T)$ are shown in Figs. 4 and 5 for two essential temperature subranges 20–75 and 75–95 K. The surface resistance of pure copper at the same frequency is shown for comparison. As it was expected, the low temperature R_s behavior was found to be similar for all the samples. It is approximately linear. The slope of linear fit of experimental curves is almost constant. The low temperature peak of R_s, which is frequently detected at lower frequencies mainly for single crystals, e.g. [2], was not observed for the ma-

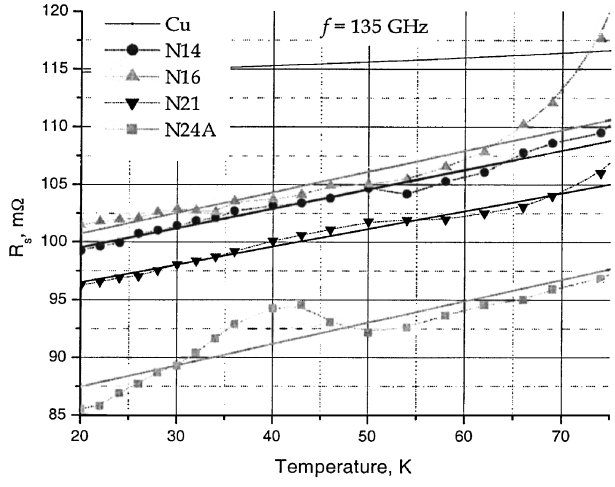

Fig. 5. Surface resistance of YBCO films in the low temperature range.

jority of samples. Only one sample (N24A) of more than 10 under the study showed a small peak at ~40 K. It is should be noted that this sample had the lowest R_s and presumably the smallest concentration of dislocations. The predominant mechanism of microwave losses could be different for this sample from the other ones.

The width of the transition, that is R_s near T_c, is significantly different for different samples. The sample N16, mentioned above as probably having the highest number of dislocations, shows the widest transition and the highest R_s. We suggest that this is a confirmation of the heat instability induced by linear defects.

A similar heat transfer problem was earlier considered in [12]. The principal considerations are as follows. The thermal conductivity equation for the film on a substrate, which is carrying resistive current, is

$$K\frac{\partial^2 T}{\partial_{\vec{r}^2}} + q(T,\vec{r}) - w(T,\vec{r}) = c\cdot\frac{\partial T}{\partial t}, \qquad (2)$$

where K is the film thermal conductivity, $q(T,r)$ is the resistive heat generation, $w(T,r)$ is the heat removal, and c is the heat capacity of the film. Since microwave currents, especially superconducting, flow mainly at the edges of film strips, the problem reduces to a quasi-one-dimensional one. Heat generation can be expressed as

$$q(T,\vec{r}) = \frac{1}{2}\cdot\frac{R_s(T,\vec{r})\cdot j^2}{d}, \qquad (3)$$

where d is the film thickness and j is the current density. The heat removal has to be integrated in two dimensions. This approximately gives

$$w(T,\vec{r}) = \frac{k(\vec{r})}{d_{\text{eff}}\cdot d}\cdot(T-T_0), \quad d_{\text{eff}} \cong \frac{b}{\pi}\cdot\ln\left(\frac{2h}{b}\right), \qquad (4)$$

where $k(\vec{r})$ is the substrate local thermal conductivity, b is the width of the region where the current flows, i.e., it should be about the London penetration depth. The characteristic current density j_p of the thermal domain propagation can be obtained by solving the following equations numerically:

$$w(T_m(j_p)) - q(T_m(j_p),\, j_p) = 0, \qquad (5)$$

$$\int_{T_0}^{T_m(j_p)} K\cdot[w(T) - q(T(j_p),\, j_p)]dT = 0, \qquad (6)$$

T_m is the maximum local temperature.

At $j < j_p$ all fluctuations collapse, but the current exceeding j_p causes destruction of the superconducting state.

However, the thermal instability can develop in the film and result in an increase of microwave losses, only when there is an sufficient initial discontinuity in the film. Moreover, the perturbation must satisfy certain conditions. Firstly, a characteristic dimension of the discontinuity has to be comparable with a heat relaxation length, that is the some characteristic length of the heat transfer problem:

$$\lambda_h = \left[K^{-1}\cdot\left.\frac{\partial f(T)}{\partial T}\right|_{T_0}\right]^{0.5}, \qquad (7)$$

where $f(T) = w(T) - q(T)$. The estimation for λ_h gives

$$\lambda_h = \sqrt{\frac{K_{\text{film}}}{K_{\text{substrate}}}\cdot d_{\text{eff}}\cdot d} \approx 50\text{ nm}. \qquad (8)$$

Such rather large value is just four times larger than the size of a normal phase region in a vicinity of the single dislocation described above. A dislocation array in a boundary between domains in quasi-single-crystal films may contain much larger number of closely spaced dislocations, which can be considered as a single discontinuity.

Secondly, the heat generation in normal phase region near a dislocation (or array) must be strong enough. Considering 2D heat balance for the stationary problem, one can calculate a local overheating ΔT due to a single dislocation:

$$\frac{1}{2}\rho_n j^2 Ld = 2\pi\lambda_h\frac{k}{d_{\text{eff}}\cdot d}\Delta T, \qquad (9)$$

$$\Delta T = \frac{\rho_n j^2 Ld}{4\pi k}. \qquad (10)$$

Of course, the resistivity ρ_n in the defect region is not known exactly, but it for sure can exceed $10^{-5}\ \Omega\cdot$m. Then, for $j \approx 3\times10^6$ A/cm^2 $\Delta T \approx 0.1$–1.0 K. This is not enough to induce a heat instability, but ΔT linearly depends on the linear size of discontinuity L. This means that a single dislocation can not have strong effect, but dislocation arrays observed experimentally can induce the thermal instability, if edge dislocations in the arrays are spaced closer than λ_h. The effect of dislocation ordering is schematically illustrated in Fig. 6. It is seen that the dislocation boundary provides much higher local temperature perturbation than separate randomly distributed dislocations.

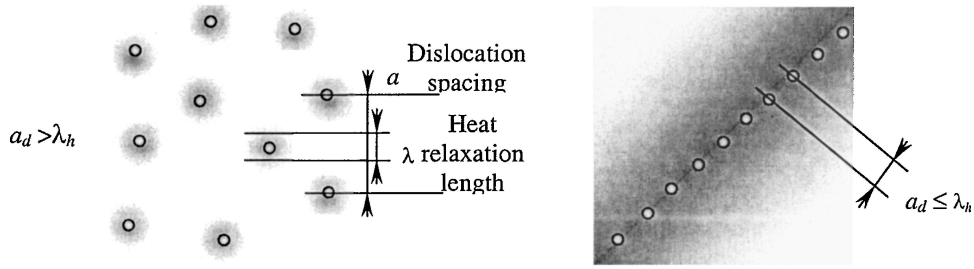

a) Random distribution of dislocations b) Dislocation array of a domain wall

Fig. 6. The diagram of temperature distribution in YBCO film carrying microwave current for random distribution of dislocations (a) and for dislocation arrays in a low angle domain boundary (b). Small circles schematically show dislocations. Shading indicates the local temperature: the darker the higher temperature.

4. CONCLUSIONS

The correlation between the defect structure and microwave properties have been revealed experimentally. Out-of-plane edge dislocations are suggested to play a remarkable role in the value and temperature behavior of the microwave surface resistance of highly biaxially oriented epitaxial YBCO films. The effect of linear defects is the most significant just below the superconducting transition. Dislocation arrays in the low-angle domain boundaries could be a source of an initial thermal fluctuation, but single dislocations can not have essential influence. Large number of linear defects (dislocations) may suppress peak of $R_s(T)$ at low temperatures due to alternative mechanism of microwave losses.

ACKNOWLEDGMENTS

This work was supported in part by the INTAS Grant 99–585 and by the Science and Technology Centre of Ukraine Project 1455.

REFERENCES

1. A. V. Velichko, M. J. Lancaster, R. A. Chakalov, and F. Wellhofer, *Phys. Rev. B* **65**, 104522 (2002).
2. R. Harris, A. Hosseini, S. Kamal, P. Dosanjh, R. Liang, W. N. Hardy, and D. A. Bonn, *Phys. Rev. B* **64**, 064509 (2001).
3. D. A. Bonn, P. Liang, and W. N. Hardy, *Phys. Rev. Lett*. **68**, 2390 (1992).
4. T. Jacobs, *Phys. Rev. Lett*. **75**, 4516 (1995).
5. J. Halbritter, *J. Appl. Phys*. **68**, 63 (1992); J. Halbritter, *J. Supercond*. **8**, 691 (1995).
6. N. Klein, *IEEE Trans. Appl. Supercond*. **3**, 1102 (1993).
7. V. M. Pan, A. L. Kasatkin, V. L. Svetchnikov, V. A. Komashko, A. G. Popov, A. Yu. Galkin, H. C. Freyhardt, and H. W. Zandbergen, *IEEE Trans. Appl. Supercond*. **9**, 1535 (1999).
8. O. Karasevska, V. Pet'kov, E. Bersudskiy, and B. Il'shin, *Ind. Lab.* No. 3, **18** (1995) (in Russian).
9. V. M. Pan, V. S. Flis, O. P. Karasevska, V. I. Matsui, I. I. Peshko, V. L. Svetchnikov, M. Lorenz, A. N. Ivanyuta, G. A. Melkov, E. A. Pashitskii, and H. W. Zandbergen, *J. Supercond.: Inc. Novel Magn*. **14**, 105 (2001).
10. V. Svetchnikov, V. Pan, Ch. Traeholt, and H. Zandbergen, *IEEE Trans. Appl. Supercond*. **7**, 1396 (1997).
11. A. Gurevich and E. A. Pashitskii, *Phys. Rev. B* **57**, 13878 (1998).
12. E. Vernoslova, K. Titkov, M. Sitnikova, and I. Vendik, *Modeling Thermal Destruction of Superconductivivity Caused by Structure Defects in HTS Film and Dielectric Substrate*, Preprint (presented at ASC 2000).